STUDIA UNIVERSITATIS BABEŞ-BOLYAI, CHEMIA, XLVIII, 2, 2003

NANOTUBE COVERING MODIFICATION

MIRCEA V. DIUDEA

Faculty of Chemistry and Chemical Engineering
"Babes-Bolyai" University, 400028 Cluj, ROMANIA
E-mail: diudea@chem.ubbcluj.ro

ABSTRACT. Nanotube tiling can be modified, from the polyhex [6] to [4, 8] and [5, 7] coverings, by following various routes for the well-known Stone-Wales SW edge rotation. The interchanging of Z[6] to A[6] and vice-versa is, for the first time, shown to proceed *via* an R[4, 8] intermediate, by SW isomerization. A new "azulenic" [5, 6, 7] covering is proposed. Isomerization routes are given in terms of edge-rotating operators, *i.e*., lattice row-column numbers associated to the edge endpoints of the repeat units in the parent net.

INTRODUCTION

Nanotubes are uni-dimensional carbon allotropes, tessellated entirely by hexagons and thus being closest to the graphite among all the graphitoids. They are obtained from graphite by several techniques,[1-3] and show unusual properties (electronic, optical, mechanical, catalytic or capillarity), with no known analogy in nature. An intensive experimental and theoretical research on nanotubes is nowadays developing. Carbon nanostructures became part of real chemistry: they have been functionalized or inserted in supramolecular assemblies.

A Stone-Wales[4] edge rotation is illustrated in Figure 1. The SW-edge (in bold) shares two cycles of size (s_m, s_n) to be reduced, after rotation, to (s_{m-1}, s_{n-1}). Correspondingly, the two cycles joined by the SW-edge will increase their size from (s_p, s_r) to (s_{p+1}, s_{r+1}).

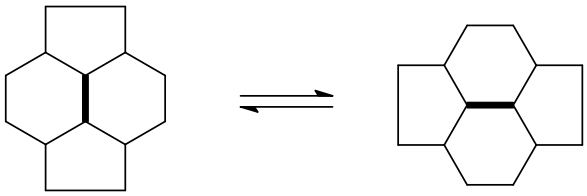

Figure 1. *Pyracylenic (Stone-Wales) isomerization*

This paper presents some isomerization ways of [6] lattice, embedded in the cylinder, leading to some more energy rich nets, seen as possible intermediates in recovering the parent [6] structure, eventually in its pairing embedding isomer. Isomerization routes, leading to known or new coverings are also presented.

ISOMERIZING [6] NANOTUBES

Covering[5] transformation is one of the ways in understanding chemical reactions occurring in fullerenes.[6-8]

Let Z[6] be embedded in the cylinder, as $ZC_6[c, n]$, or the “zig-zag" ($c/2$, 0) nanotube,[9-11] Figure 2. Similarly, the embedding of A[6] is $AC_6[c, n]$, and the nanotube is called “armchair", Figure 3.

Let denote by $H_{(i,j),(p,r)}$ the edges lying parallel to the horizontally oriented tube generator, in the schematic lattice representation; the first subscript bracket encodes the relative location of the start-point of rotating edges along the tube while the second one the location of edges around the tube. Mark $V_{(i,j),(p,r)}$ the edges lying perpendicular to the tube generator. The marked edges will be rotated in the following isomerization and the above symbols play the role of a true rotational operator, as shown in the following.

The polyhex [6] covering is transformed into the “rhomboidal-bathroom-floor" tiling[12] R[4, 8], by operations:

$$H_{(1,3),(1,3)}(Z[6]) = R[4, 8] = V_{(1,3),(1,3)}(A[6]) \quad (1)$$

and the corresponding products are illustrated in Figures 2 and 3. The starting objects in these figures represent pair isomers of different embeddings, in the cylinder, of the same net having 16 x 8 = 128 atoms.

$H_{(1,3),(1,3)}$ (ZC_6[16,8]) RC_4C_8[16,8]

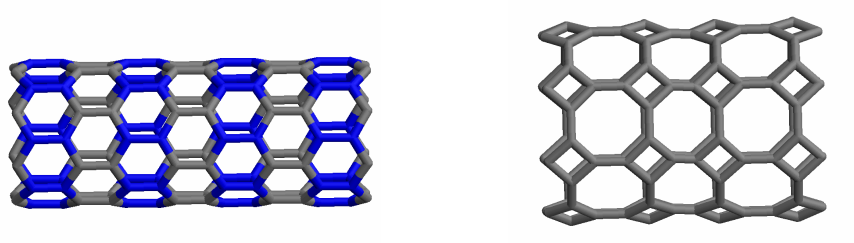

Figure 2. *A ZC_6 nanotube of 128 atoms and its SW isomer.*

When the SW isomerization follows a spiral path, like that illustrated in Figure 4, the product is, after optimization by an MM procedure, a “squared-bathroom-floor" $SC_4C_8[c, n]$ lattice.[13] The operation can be written as:

$$V_{(1,5),(1,5)}(Z[6]) = S[4, 8] \quad (2)$$

Similarly, the operation:

$$V_{(1,5),(1,5),1a}(Z[6]) = SP[5, 7] \quad (3)$$

leads to a spiral $SPC_5C_7[c, n]$ net,[14] Figure 5. Note the combination *V*& *Z*, for describing a spiral path and the subscript *1a* for a “leave one row/column out" way in getting an “alternating" spiral net.

$V_{(1,3),(1,3)}$ (AC_6[8,16]) RC_4C_8[8,16]

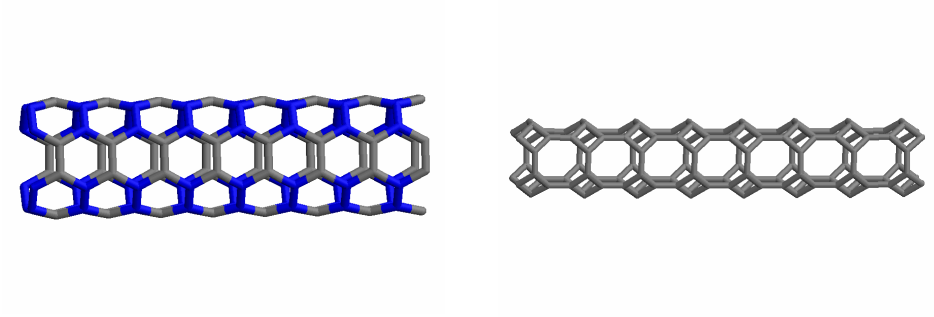

Figure 3. *An AC_6 nanotube of 128 atoms and its SW isomer.*

$V_{(1,5),(1,5)}$(ZC_6[16,8]) SC_4C_8[16,8]

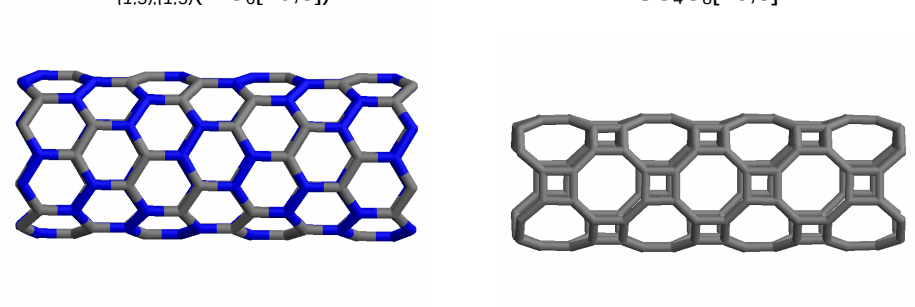

Figure 4. *A spiral path of SW edge rotation*

The same operations can be done by the A[6] net thus resulting the corresponding pair embedding isomers.

Different azulenic [5, 7] lattices can be obtained by the following operations:

$$H_{(1,5),(1,5)}(Z[6]) = V[5, 7] \quad (4)$$

$V_{(1,5),(1,5),1a}$ (ZC_6[16,8]) SPC_5C_7[16,8]

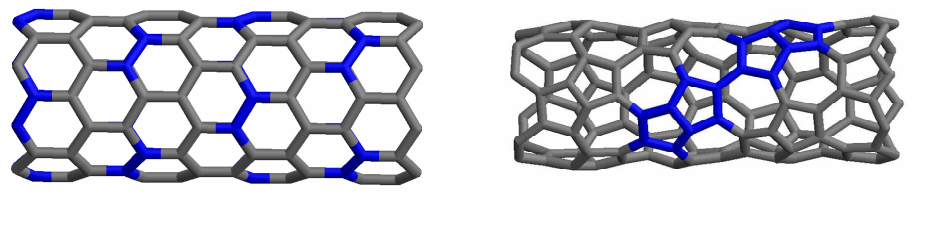

Figure 5. *A spiral path of SW edge rotation and its spiral net product*

$$V_{(1,5),(1,5)}(A[6]) = H[5, 7] \quad (5)$$

These coverings will be illustrated in the next section.

ISOMERISING [4, 8] NANOTUBES

The [4, 8] covering, particularly R[4, 8], transforms to either AC_6 or ZC_6 net by operations:

$$H_{(1,4),(1,4)}(R[4, 8]) = A[6] \quad (1`)$$

$$V_{(1,4),(1,4)}(R[4, 8]) = Z[6] \quad (1``)$$

as a unique intermediate of the [6] net isomerization (the different embeddings disregarded).

Other isomerizations of this covering are:

$$H_{(1,7),(1,7)}\ (R[4, 8]) = H[5, 7] \quad (6)$$

$$V_{(1,7),(1,7)}\ (R[4, 8]) = V[5, 7] \quad (7)$$

the corresponding objects being illustrated in Figure 6. Note that the pentaheptite H/V[5, 7] lattice is encountered in the chemical net of ThMoB4.[15] It is a *2-isohedral* tiling,[16] (*i.e.*, it has only two face orbits), with the local signature (t_5, t_7) = (1, 3), meaning every pentagon has t_5 pentagonal neighbors and every heptagon has t_7 heptagonal neighbors. Crespi *et al*.[17] have stated that such nanotubes would be metallic.

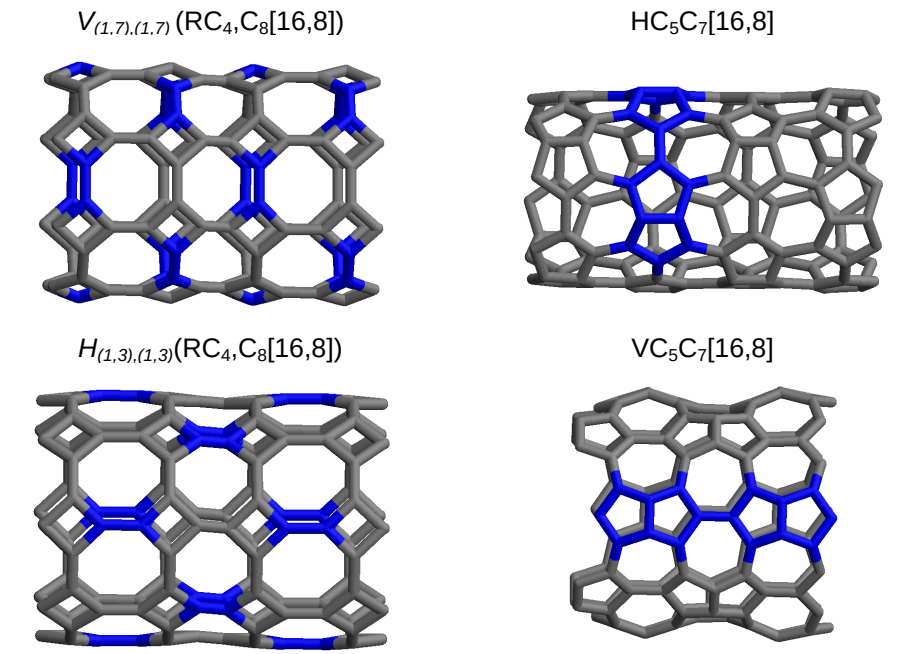

Figure 6. *SW isomerization of RC_4,C_8[16,8] resulting two embedding isomers of the H/V[5, 7] lattice.*

Other combinations of SW rotation, on R[4, 8], are as follows:

$$V_{(1,3),(1,6)}(H_{(1,4),(1,7)}(\mathrm{R}[4, 8])) = \mathrm{HA}[5, 7] \quad (8)$$

$$H_{(1,6),(1,3)}(V_{(1,7),(1,4)}(\mathrm{R}[4, 8])) = \mathrm{VA}[5, 7] \quad (9)$$

the objects being presented in Figures 7 and 8, respectively. The net is a *2-isohedral* tiling and has the signature [2, 4]. It is a periodic (*i.e.*, face-regular) covering, described as capped tubulenes elsewhere.[18]

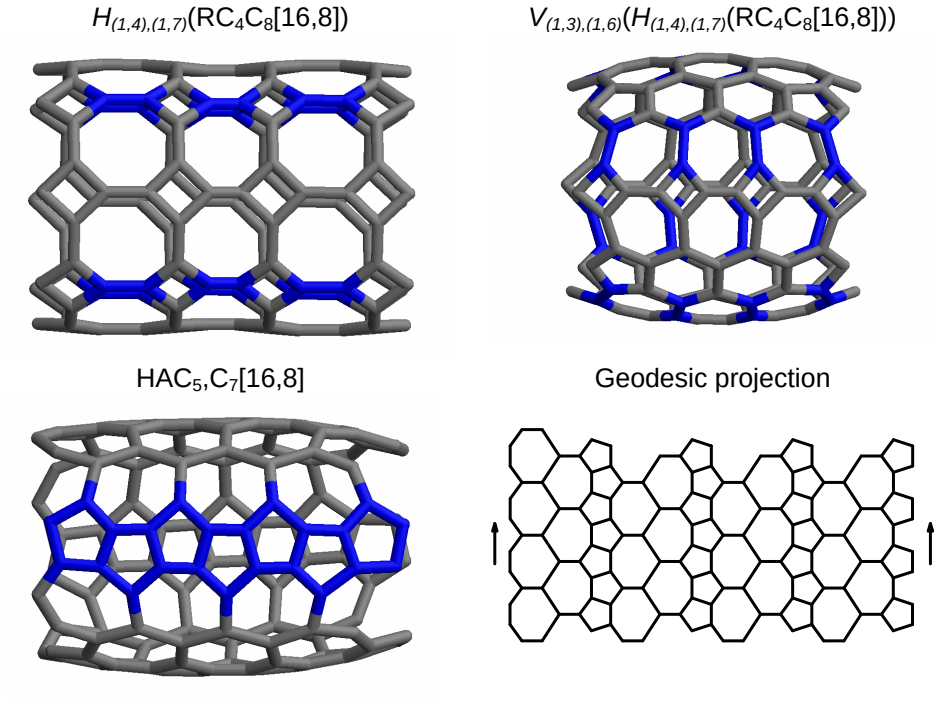

Figure 7. *The pathway to HA[5, 7] lattice.*

Geodesic projections are useful in understanding the connectivity in a lattice embedded in a given surface.

Other isomerizations are derivable form the above ones:

$$V_{(1,5),(1,6)}\,(H_{(1,4),(1,7)}(\mathrm{R}[4, 8])) = \mathrm{HA}[5, 6, 7] \quad (10)$$

$$H_{(1,6),(1,5)}\,(V_{(1,7),(1,4)}(\mathrm{R}[4, 8])) = \mathrm{VA}[5, 6, 7] \quad (11)$$

and the objects are presented in Figures 9 and 10. This novel lattice has the local signature: $t_{5j}(0, 4, 1)$; $t_{6j}(2, 2, 2)$; and $t_{7j}(1, 4, 2)$, $j = 5, 6, 7$. It is a “fully azulenoid" covering, in the terminology of Kirby.[19]

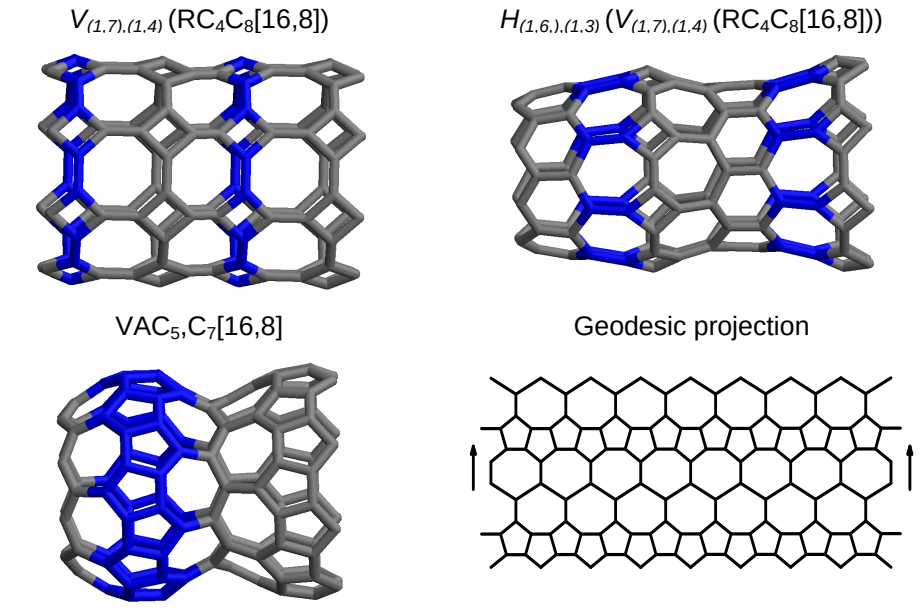

Figure 8. *The pathway to VA[5, 7] lattice.*

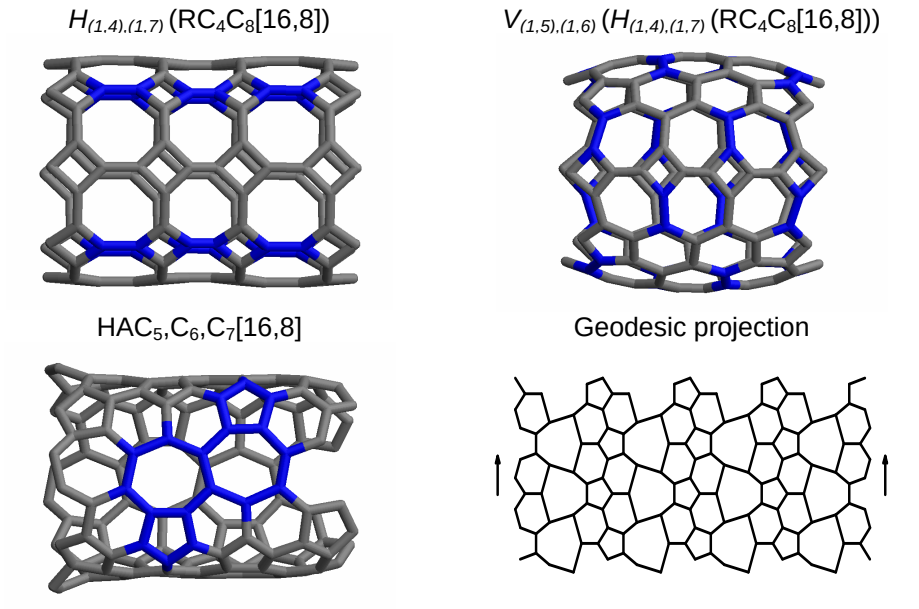

Figure 9. *The pathway to HA[5, 6, 7] lattice.*

Note that the [4, 8] lattices are deductible from the primary square covering, embedded in the cylinder, by some basic operations on maps.[20, 21] Such non-chemical transformations will be discussed in a future paper.

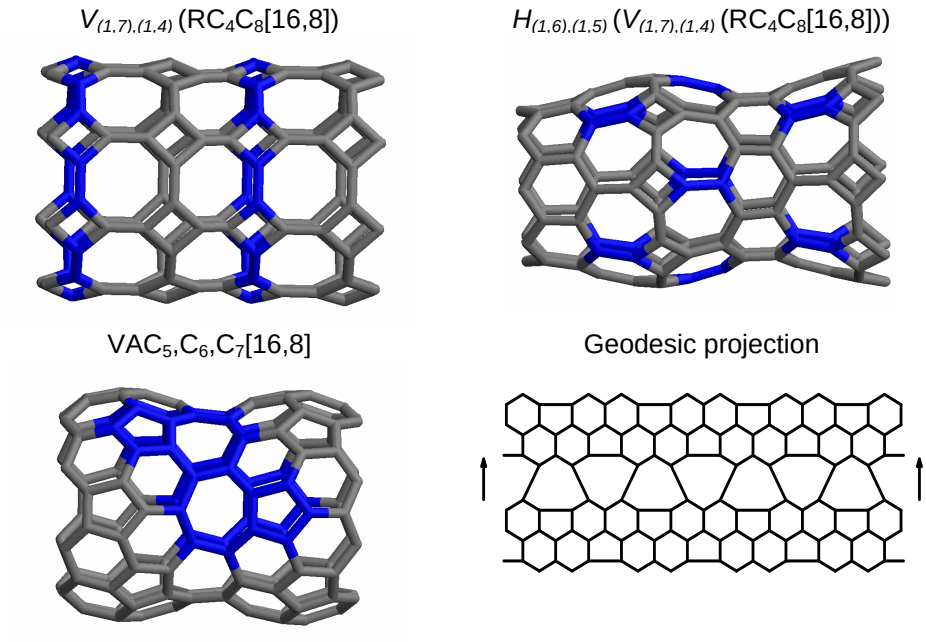

Figure 10. *The pathway to VA[5, 6, 7] lattice.*

ENERGETICS AND SPECTRAL PROPERTIES

In the simple Hückel molecular orbital HMO theory,[22] the energy of the i^{th} molecular orbital $E_i = \alpha + \lambda_i \beta$ is calculated from the eigenvalues λ_i of the adjacency matrix associated with the molecular hydrogen-depleted graph. The π-electronic shells of neutral molecules are classified, according to their eigenvalue spectra, as:[23] (i) *properly closed*, PC, when $\lambda_{N/2} > 0 \geq \lambda_{N/2+1}$; (ii) *pseudo-closed*, PSC, when $\lambda_{N/2} > \lambda_{N/2+1} > 0$ and (iii) *open*, OP, when HOMO-LUMO molecular orbitals are degenerate, $\lambda_{N/2} = \lambda_{N/2+1}$ and the HOMO-LUMO gap (taken as the absolute value of the difference E_{HOMO} - E_{LUMO}, in $|\beta|$ units) vanishes.

The metallic M character (a property taken from the Solid State Physics) is associated with an open shell π-electronic structure having four non-bonding orbitals (NBOs = zero eigenvalues), a condition reached by the graphite sheet and some tori and nanotubes.[24]

The spectral data of the herein discussed nanotubes are listed in Table.

As shown in Table, various coverings provide different π-electronic shells. Their π-energy E_π is calculated as:[25]

$$E_\pi = \alpha \cdot n_e + \beta \cdot \sum_{i=1}^{N} g_i \cdot \lambda_i \qquad (6)$$

where α and β are the standard HMO parameters, n_e is the number of π-electrons, while g_i is the occupation number of the i^{th} molecular orbital.

Table

Spectral properties and energy per atom: E_π (|β|) and E-MM (kcal/mol).

	Structure	$HOMO_{-1}$	HOMO	LUMO	$LUMO_{+1}$	Gap	Shell	E_π	E-MM
1	AC_6[8,24]	0.148	0.072	-0.072	-0.148	0.143	PC	1.550	3.567
2	ZC_6[16,12]	0.017	**0**	**0**	-0.017	0.000	OP	1.542	2.444
3	VC_5C_7[8,24]	0.184	0.139	0.107	0.048	0.032	PSC	1.510	6.939
4	HC_5C_7[16,12]	0.212	0.198	0.141	0.141	0.057	PSC	1.501	4.059
5	HC_5C_7[8,24]	0.187	0.121	0.121	0.099	0	OP	1.514	8.903
6	SPC_5C_7[16,12]	0.202	0.093	0.093	0.018	0.000	OP	1.507	5.045
7	SC_4C_8[16,12]	0.042	0.042	-0.042	-0.042	0.084	PC	1.455	11.185
8	RC_4C_8[16,12]	**0**	**0**	**0**	**0**	**0**	**M**	1.441	10.641
9	RC_4C_8[8,24]	**0**	**0**	**0**	**0**	**0**	**M**	1.454	14.325
10	HAC_5C_7[16,12]	0.184	0.018	0.018	0	0	OP	1.499	6.705
11	$HAC_5C_6C_7$[16,12]	**0**	**-0.004**	**-0.004**	**-0.029**	**0**	**OP**	1.508	**3.373**
12	C_{60}	0.618	0.618	-0.139	-0.139	0.757	PC	1.553	4.460

The total π-electron energy, has a topological essence by the spectral parameter λ_i. Taking $\alpha = 0$ (the reference energy) and $\beta = 1$ (the unity energy), it is immediate $E_\pi = \lambda_i$. It has been shown[26] that E_π is proportional not only to the π-, but also the σ-electron energy of the C-C bonds. In the absence of large steric strain in the carbon skeleton, E_π can be used for calculating several thermodynamic functions of chemical compounds. In the case of conjugated benzenoid hydrocarbons, the enthalpies calculated by using the total π-electron energy have been found closer to the experimental values than the values computed by some highly parametrized molecular-mechanics MM and semiempirical procedures.[25]

The "topological resonance energy" TRE of Aihara[27-29] and Gutman *et al*.[30,31] is defined as the difference $E_\pi - E_{ref}$ between the total π-energy of a conjugated (aromatic) system and the energy of some reference structures (also calculated by a topological background). The systems having TRE > 0 are classified as "aromatic", those having TRE < 0 as "antiaromatic" while those for which TRE ≈ 0 as "non-aromatic". Figure 10 illustrates the plot of the π-energy *vs* the MM+ energy of the herein discussed nanotubes.

Keeping in mind the (-) sign of β parameter, the plot in Figure 10 clearly indicates a proportionality between E_π and the total MM+ energy, which accounts for the energy of σ-frame rather than for that of π-electrons.

The A[6] covering (Table, entry 1), appears to be the most aromatic structure (compare with C_{60}, Table, entry 12), even though the MM energy of its open nanotube embedding is somewhat higher than that corresponding to Z[6] (Table, entry 2). This is due to a higher strain energy of its σ-frame.

The next are the pentaheptite [5, 7] lattices (Table, entries 3-6), for which "azulenic" polarization is expected. The same comments as for A[6] are true for V[5, 7] in the sub-set of azulenic nets. As above mentioned, the tubes $H/VC_5,C_7$ are expected to be metallic; our results indicate this character is conditioned by the tube dimensions (particularly the *c*-dimension – see the PSC/OP variation of their shell - Table).

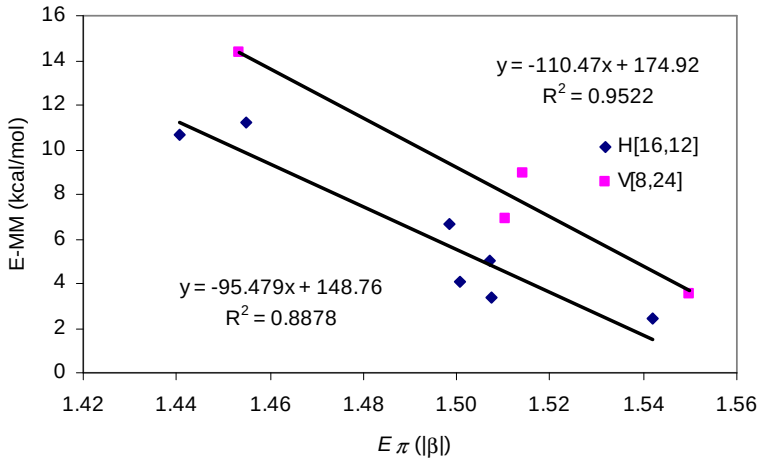

Figure 10. *The plot of the π-energy vs the MM+ energy in nanotubes of various covering*

The [4, 8] coverings (Table, entries 8 and 9) show the lowest stability among the lattices herein discussed. The most interesting seems the R[4, 8] net, capable to isomerize in all but spiral discussed lattices. It has a metallic π-shell and the lowest E_π suggesting no conjugation, a normal fact for an anti-aromatic structure.

An intriguing electronic structure shows $HAC_5C_6C_7$[16,12] (Table, entry 11), which frontier orbitals are antibonding (near non-bonding) and degenerate. Its low E_π could be explained by the "azulenic" conjugation of the isolated C_5C_7 pair as well as by the low strain energy of its skeleton, relaxed by means of the negatively curved heptagons (see the low value of MM energy). Note that the $HAC_5C_6C_7$[12,4] repeat unit can be capped by two hexagons to give the fullerene C_{60}; thus, the tube $HAC_5C_6C_7$[12,*n*] is a true C_{60}-like periodic nanostructure. Their electronic properties depend, however, of the tube dimensions.

Molecular modeling was performed on a 2x1GHz Pentium III PC using the MM+ force field, with the parametrization supplied by HyperChem software (version 4.5, Hypercube, Inc.).[32] Structures were optimized by using the Polak-Ribier conjugate-gradient method, the energy minimization was terminated at an RMS gradient <0.01 kcal/(Å·mol) for all structures. Spectral data were calculated by the TOPOCLUJ software package.[33] The Stone-Wales edge rotations have been performed by the CageVersatile 1.1 original program.[34]

CONCLUSIONS

The coverings herein discussed all are face-regular or periodic structures. Nanotube tiling can by modified from the polyhex [6] to [4, 8] which seems to be a crucial intermediate between pure [6] and mixed [5, 7], [5, 6, 7] etc. The Stone-Wales SW edge rotation is the tool that makes possible the tiling modification. As shown elsewhere,[7] cascade SW rotations are true chemical reactions and their products have to be looked for in the soot of vaporized graphite.

Acknowledgement. This paper was supported by a Romanian CNCSIS 2003 GRANT.

REFERENCES

1. M. Endo, S. Iijima and M. S. Dresselhaus, *Carbon Nanotubes*, Pergamon, **1996**.
2. M. S. Dresselhaus, G. Dresselhaus, and P. C. Eklund, *Science of fullerenes and carbon nanotubes*, Acad. Press, San Diego, **1996**.
3. K. Tanaka, T. Yamabe, and K. Fukui, *The science and technology of carbon nanotues*, Elsevier, **1999**.
4. A. J. Stone and D. J. Wales, *Chem. Phys. Lett.* **1986**, *128*, 501-503.
5. B. Grünbaum and G. C. Shephard, *Tilings and Patterns*, Freeman, New York, **1985**.
6. D. J. Klein and H. Zhu, in: A. T. Balaban, (Ed.), *From Chemical Topology to Three - Dimensional Geometry*, Plenum Press, New York, **1997**, pp. 297-341.
7. Y. Zhao, B. I. Yakobson, and R.E. Smalley, *Phys. Rev. Lett*., **2002**, *88,* 185501.
8. M. Deza, P. W. Fowler, M. Shtorgin, and K. Vietze, *J. Chem. Inf. Comput. Sci.*, **2000**, *40*, 1325-1332.
9. A. L. Ivanovskii, *Russ. Chem. Rev.*,**1999**, *68*, 103-118.
10. M. V. Diudea, O. Ursu, and B. Parv, *Studia Univ. "Babes-Bolyai"*, **2003**, *48*, 11-20.
11. M. V. Diudea, T. S. Balaban, E. C. Kirby, and A. Graovac, *Phys. Chem., Chem. Phys.*, **2003** (in press).
12. M. Stefu and M. V. Diudea, *MATCH Commun. Math. Comput. Chem*., **2003** (in press).
13. M. V. Diudea, B. Parv, P. E. John, O. Ursu, and A. Graovac, *MATCH Commun. Math. Comput. Chem*., **2003**, *49*, 23-36.
14. M. V. Diudea, B. Parv, and E. Kirby, E. C. *MATCH Commun. Math. Comput. Chem*., **2003**, 47, 53-70.
15. M. O'Keeffe and B. G. Hyde, *Crystal Structures*, Mineralogical Society of America, Washington DC, **1996**.
16. B. Grünbaum, H. D. Löckenhoff, G. C. Shephard, and A. Temesvari, *Geom. Dedicata*, **1985**, *19*, 109-174.
17. V. H. Crespi, L. X. Benedict, M. L. Cohen, and S. G. Louie, *Phys. Rev. B* , **1996**, *53*, 13303-13305.
18. M. V. Diudea, I. Silaghi-Dumitrescu, and A. Graovac, *Croat. Chem. Acta*, **2003** (submitted).
19. E.C. Kirby, *MATCH Commun. Math. Comput. Chem.* **1996**, *33*, 147-156.
20. M. V. Diudea, P. E. John, A. Graovac, M. Primorac, and T. Pisanski, *Croat. Chem. Acta*, **2003**, *76*, 153-159.
21. M. V. Diudea, *PCCP*, **2002**, *4*, 4740-4746.
22. E. Hückel, *Z. Phys.*, **1931**, *70***,** 204-286.
23. P. W. Fowler and T. Pisanski, *J. Chem. Soc*., *Faraday Trans*., **1994**, *90*, 2865-2871.
24. M. Yoshida, M. Fujita, P. W. Fowler, and E. C. Kirby, *J. Chem. Soc., Faraday Trans*., **1997**, *93*, 1037-1043.
25. I. Gutman and Y. Hou, *MATCH Commun. Math. Comput. Chem*., **2001**, *43*, 17-28.
26. L. J. Schaad and B. A. Hess, *J. Am. Chem. Soc*., **1972**, *94*, 3068.
27. J. Aihara, *J. Am. Chem. Soc*., **1976**, *98*, 2750-2758.
28. J. Aihara, *J. Mol. Struct.* (*Theochem*), **1994**, *311*, 1-8.
29. J. Aihara, D.Babic and I. Gutman, *MATCH Commun. Math. Comput. Chem*., **1996**, *33*, 7-16.
30. I. Gutman, M. Milun, and N. Trinajstic, *MATCH Commun. Math. Comput. Chem.*, **1975**, *1,* 171-175.
31. I. Gutman, M. Milun, and N. Trinajstic, *J. Am. Chem. Soc*., **1977**, *99*, 1692-1704.
32. HyperChem [TM], release 4.5 for SGI, © **1991-1995**, Hypercube, Inc.
33. M. V. Diudea, O. Ursu, and Cs. L. Nagy, TOPOCLUJ, "Babes-Bolyai" University, Cluj, **2002**.
34. M. V. Diudea and M. Stefu, CageVersatile CV 1.1, "Babes-Bolyai" University, Cluj, **2003**.